JOURNAL OF GEOPHYSICAL RESEARCH, VOL. 112, A07303, doi:10.1029/2007JA012283, 2007

Yearly variations of global plasma densities in the topside ionosphere at middle and low latitudes

Libo Liu,[1] Biqiang Zhao,[1] Weixing Wan,[1] S. Venkartraman,[2] Man-Lian Zhang,[1] and X. Yue[1]

Received 18 January 2007; revised 24 February 2007; accepted 10 April 2007; published 13 July 2007.

[1] In this paper, the 10-year (1996–2005) measurements of total ion density (N_i) from the Defense Meteorological Satellite Program (DMSP) spacecraft at 0930 and 2130 LT have been analyzed to investigate the yearly variations of global plasma densities in the topside ionosphere at magnetic latitudes from 60°S to 60°N. Results indicate that there are strong yearly variations in the DMSP N_i at 840 km. The annual components of longitude-averaged N_i dominate at most latitudes with maxima around the June solstices in the Northern Hemisphere and the December solstice in the Southern Hemisphere. In contrast, seasonal anomaly (maxima N_i around the December solstice) exists in the northern equatorial zone. Moreover, the differences in N_i at the two solstices are not symmetrical about the magnetic equator, being generally higher in the Southern Hemisphere than in the Northern Hemisphere. Conjugate-averaged N_i is substantially greater at the December solstice than at the June solstice. This annual asymmetry is modulated by solar activity effect and has latitudinal and longitudinal structures. The longitude effects of the annual asymmetry depend on local time, being stronger in the evening sector than in the morning sector. The solstice differences and annual asymmetry are more marked with increasing solar activity. The annual asymmetry appears not only in the rising phase of the solar cycle but also in the declining phase. Thus the solar condition differences between the two solstices do not account for the N_i asymmetry. The concentration of neutral oxygen [O], provided from the NRLMSIS model, shows a similar pattern of annual and hemispheric asymmetries. Moreover, effects of the HWM model neutral winds are also constituent with the change patterns of N_i. Therefore, considering the principal processes in the topside ionosphere, the changes of [O] and the rates of thermospheric winds should contribute to the annual asymmetry in N_i at 840-km altitude.

Citation: Liu, L., B. Zhao, W. Wan, S. Venkartraman, M.-L. Zhang, and X. Yue (2007), Yearly variations of global plasma densities in the topside ionosphere at middle and low latitudes, *J. Geophys. Res.*, *112*, A07303, doi:10.1029/2007JA012283.

1. Introduction

[2] It is well known that the temporal and spatial variations of the Earth's ionosphere at and above the peak of the F_2 layer behave differently from the solar zenith angle dependence as predicted by the Chapman ionization theory [e.g., *Bailey et al.*, 2000; *Balan et al.*, 1998, 2000; *Gulyaeva and Rawer*, 2003; *Mendillo et al.*, 2005; *Richards*, 2001; *Rishbeth*, 1998; *Rishbeth et al.*, 2000; *Rüster and King*, 1973; *Su et al.*, 1998; *Torr and Torr*, 1973; *Torr et al.*, 1980; *Wright*, 1963; *Yonezawa*, 1971; *Zhang et al.*, 2005; *Zou et al.*, 2000]. Historically, when the observed behaviors of the F_2 layer were significantly deviated from the predicted solar zenith angle dependence, they were called "anomalies." Typical examples of these anomalies in the F_2 layer are the so-called "seasonal anomaly" or "winter anomaly" (that the daytime values of midlatitude N_mF_2 in the Northern Hemisphere are much greater in winter than in summer), "annual anomaly" or "nonseasonal anomaly" (take the Northern and Southern Hemispheres in the world as a whole N_mF_2 in December is greater than in June during both the daytime and at night), "semiannual anomaly" (greater N_mF_2 at equinox than at solstice), and "equatorial anomaly" (The equatorial anomaly is within approximately ±20° of the magnetic equator.) [e.g., *Ivanov-Kholodny and Mikhailov*, 1986; *Moffett*, 1979; *Torr and Torr*, 1973; *Torr et al.*, 1980; *Whalen*, 2003] and so on. The annual anomaly or nonseasonal anomaly is sometimes called the "annual asymmetry." Such anomalies are now attributed to variations of atmospheric compositions and/or to dynamic processes including plasma transportations because of atmospheric neutral circulations and other factors [e.g., *Bailey et al.*, 2000; *Mendillo et al.*, 2005; *Rishbeth*, 1998;

[1]Institute of Geology and Geophysics, Chinese Academy of Sciences, Beijing, China.
[2]William B. Hanson Center for Space Sciences, University of Texas at Dallas, Richardson, Texas, USA.

0148-0227/07/2007JA012283$09.00

Rishbeth et al., 2000] that were quite unknown in Chapman's time.

[3] Many assumptions have been proposed to explain the variations of the anomalies, including the "geometrical explanations," the "thermal explanations," the "chemical explanations," and so on [see *Rishbeth*, 1998; *Zou et al.*, 2000, and references therein]. Among these anomalies, the seasonal anomaly or winter anomaly may be associated with the seasonal changes of atmospheric compositions produced by a global circulation [e.g., *Duncan*, 1969; *Millward et al.*, 1996; *Rishbeth and Setty*, 1961], while causes for the annual asymmetry is still not completely understood and remains unexplained [*Mendillo et al.*, 2005]. Investigations of the annual asymmetry have used data on N_mF_2 from ionosondes [e.g., *Yonezawa*, 1971; *Rishbeth and Müller-Wodarg*, 2006] and on the total electron content (TEC) from two stations [*Titheridge and Buonsanto*, 1983], global GPS networks [*Mendillo et al.*, 2005; *Zhao et al.*, submitted manuscript, 2007], and from the TOPEX mission (*Wan et al.*, submitted manuscript, 2007). In this paper, we use a database of total ion densities (N_i) in the topside ionosphere from Defense Meteorological Satellite Program (DMSP) measurements at 840-km altitude [e.g., *Greenspan et al.*, 1994; *Rich et al.*, 2003; *Sultan and Rich*, 2001; *West et al.*, 1997], which allows us to examine the global asymmetries of the plasma densities in the topside ionosphere at middle and low latitudes.

[4] Previous studies have shown that the ionospheric variations have significant altitude dependencies [e.g., *Balan et al.*, 2000; *Fatkullin*, 1973; *Gondhalekar and King*, 1973; *Rich et al.*, 2003; *Su et al.*, 1999]; that is, the behaviors in the topside ionosphere are rather different from those in the *F* region. For example, *Su et al.* [1999] found strong altitude dependencies in the solar activity variations of electron densities, which were observed with the Japanese incoherent scatter radar. Recently, *Rich et al.* [2003] revealed that the solar rotation (27-day) effect is rather pronounced in the topside plasma density than in TEC. Furthermore, winter anomaly does not appear in the topside ionosphere [*Bailey et al.*, 2000], whereas it is found obviously in the midlatitude *F* region [*Torr and Torr*, 1973; *Yonezawa*, 1971]. Plasma densities have been observed to be higher in December than in June [*Guiter et al.*, 1995]. With the plasma density observations from the Hinotori satellite at 600-km altitude, *Su et al.* [1998] and *Bailey et al.* [2000] found strong annual anomaly in the low-latitude topside ionosphere. Hitherto, limited analyses on climatological patterns have been applied to the topside ionosphere [e.g., *Bailey et al.*, 2000; *Denton et al.*, 1999; *Rich et al.*, 2003; *Su et al.*, 1999, 2005; *West et al.*, 1997; *Zhao et al.*, 2005], compared to those at the peak of the F_2 layer.

[5] Topside plasmas were continuously measured by the Defense Meteorological Satellite Program (DMSP) spacecraft since 1987 [e.g., *Greenspan et al.*, 1994; *Rich et al.*, 2003; *Sultan and Rich*, 2001; *West et al.*, 1997]. This large data source is ideally suited for studying the climatology of plasma densities, drifts, and temperatures in the topside ionosphere, although it does not provide the necessary local time coverage. In this analysis, data from the DMSP measurements during 10 years from 1996 to 2005 are collected to investigate the yearly variations of the topside ionosphere. We will mainly focus on the annual asymmetry in the morning and evening (0930 and 2130 LT) sectors at middle and low latitudes.

2. Data Source

[6] The series of the DMSP spacecraft are designated with the letter F and the flight number, for example, F12, F14, and F15. DMSP spacecraft are in Sun-synchronous polar orbits around the 840-km altitude. The period of an orbit is about 101 min, and consecutive orbits are separated in longitude by 25.5°. The nearly constant local time of the DMSP orbital planes at middle and low latitudes makes their ionospheric measurements unique for allowing other drivers of the plasma characteristics to be more noticeable. The overlapped operational time of the spacecraft ensures the data's integrity.

[7] The spacecraft carries a "Special Sensor for Ions, Electrons, and Scintillation" (SSIES) package to monitor the behavior of thermal plasma in the topside ionosphere since 1987. This package has been described in many works [e.g., *Greenspan et al.*, 1994; *Rich et al.*, 2003; *Sultan and Rich*, 2001; *West et al.*, 1997]. The sum of plasma densities over all ion species (referred to as the total ion density or N_i) is measured with the onboard scintillation meter at a resolution of 24 Hz. In this paper, only data in the morning and evening (0930 and 2130 LT) sectors from the spacecraft F12, F14, and F15 were chosen for analysis. The N_i data are archived and provided at the University of Texas, Dallas (UTD) Web site as 4-s averages. We used the geomagnetic coordinates provided by UTD, which are the corrected geomagnetic coordinates of the subspacecraft location. At each local time sector, values of N_i are averaged in latitude bins (within a 3°-latitude window) between ±60° geomagnetic latitude in each day during the years from 1996 to 2005. Each latitude bin includes data points over all longitudes (longitude-averaged case) or over longitude sectors (specified longitude zone case). Irregularity structures, for example, equatorial plasma density bubbles, may appear in the postsunset topside ionosphere [e.g., *Huang et al.*, 2001]. We adopt the method of *Su et al.* [2006] to remove irregularities in the data set before taking the average.

[8] The 10.7-cm solar radio flux, $F_{10.7}$, is often used as a standard proxy for solar activity. In this paper, we adopt the adjusted values of $F_{10.7}$ which are provided at the SPIDR (Space Physics Interactive Data Resource) Web site in accord with the work of *Liu et al.* [2006a, 2006b], since different $F_{10.7}$ values (the observed, adjusted, and absolute values provided by the US National Geophysical Data Center) do not greatly affect our conclusions. Figure 1 shows the variations of $F_{10.7}$ and the time coverage of DMSP N_i we used. Moreover, we ignore the geomagnetic activity effects on the plasma densities in this analysis. *Zhao et al.* [2005] examined storm effects for more than a hundred cases during 1996–2004 and found that N_i is enhanced during the main phase of the storm and depressed during the recovery phase of the storm. There is no obvious statistical relationship between N_i and geomagnetic disturbances. As a matter of fact, since the topside ionosphere is

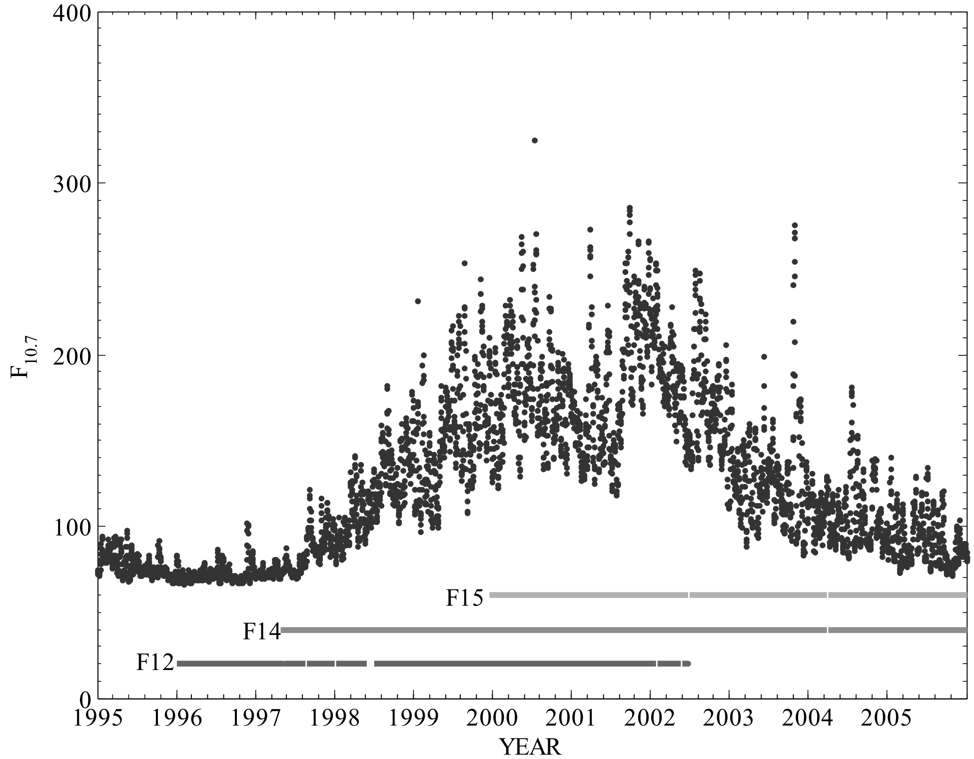

Figure 1. Time coverage of DMSP N_i with corresponding solar index $F_{10.7}$ (in 10^{-22} W·m^{-2}·Hz^{-1}).

largely controlled by the solar flux, the geomagnetic effect is less evident.

3. Results

3.1. Yearly Variations of DMSP N_i

[9] As an example to portray the yearly variations, Figure 2 shows the daily longitude-averaged DMSP N_i at magnetic latitudes ±6°, ±16°, ±32°, and ±48° at (1) 0930 and (2) 2130 LT during the years from 1996 to 2005. Red points correspond to the daily data in the Southern Hemisphere and blue points to those in the Northern Hemisphere. The vertical dashed lines show the beginnings of the years. It is obvious that DMSP N_i has distinct local time and seasonal variations and strong solar activity dependency. The hemispheric asymmetry becomes stronger with increasing solar activity.

[10] It can be seen from Figure 2 that the annual variations of longitude-averaged N_i predominate at middle and low latitudes with maxima around the June solstices in the Northern Hemisphere and around the December solstices in the Southern Hemisphere and minima 6 months out of phase (see the panels except the bottom ones). In contrast, in the equatorial zone (6°N–6°S), the values of N_i are substantially higher around the December solstices than the June solstices in both hemispheres; that is, seasonal anomaly still exists in the northern equatorial zone. The general feature is similar in both 0930 and 2130 LT sectors (see the bottom panels). Another significant feature is that there are strong solar activity modulations in the annual variation of N_i. It is evident that, with increasing solar activity, the differences of longitude-averaged N_i at both the December and June solstices are seen to be substantially larger (this can also be found in Figure 4). The solar activity features in DMSP N_i have been presented in detail by *Liu et al.*, 2007b, which found that DMSP N_i has an approximately linear dependence on daily $F_{10.7}$ and a nonlinear dependence on EUV fluxes. The linear correlation coefficients between N_i and $F_{10.7}$ at a given location and season vary from 0.6 to higher than 0.9. At the same time, the 27-day effect in N_i is rather pronounced, which has been reported in the work of *Rich et al.* [2003]. Our tests indicate that whether the 27-day variation effects be removed or not do not significantly affect the features presented in this paper.

[11] At a lower altitude (600 km), the yearly variation of the low-latitude electron density (N_e) has maxima around the equinoxes and minima around the solstices [*Bailey et al.*, 2000]. This feature, the so-called semiannual anomaly, has also been observed in the topside profiles measured by the Japanese middle and upper atmosphere (MU) radar [*Balan et al.*, 2000] and in the ionospheric *F* region and TEC. However, it is quite different at 840-km altitude that, in general, the semiannual anomaly appears only in the magnetic equatorial region at 2130 LT and is much weak or absent at higher latitudes in DMSP N_i. Thus our result confirms the existence of altitude dependence of the yearly variations.

[12] The yearly variations of N_i can be considered as a combination of the annual and semiannual components and the yearly average as follows:

$$N_i = A_{\mathrm{mean}} + A_{annual} + A_{\mathrm{semiannual}} + \varepsilon \qquad (1)$$

Where A_{mean}, A_{annual}, and $A_{\mathrm{semiannual}}$ are the corresponding yearly average and annual and semiannual components,

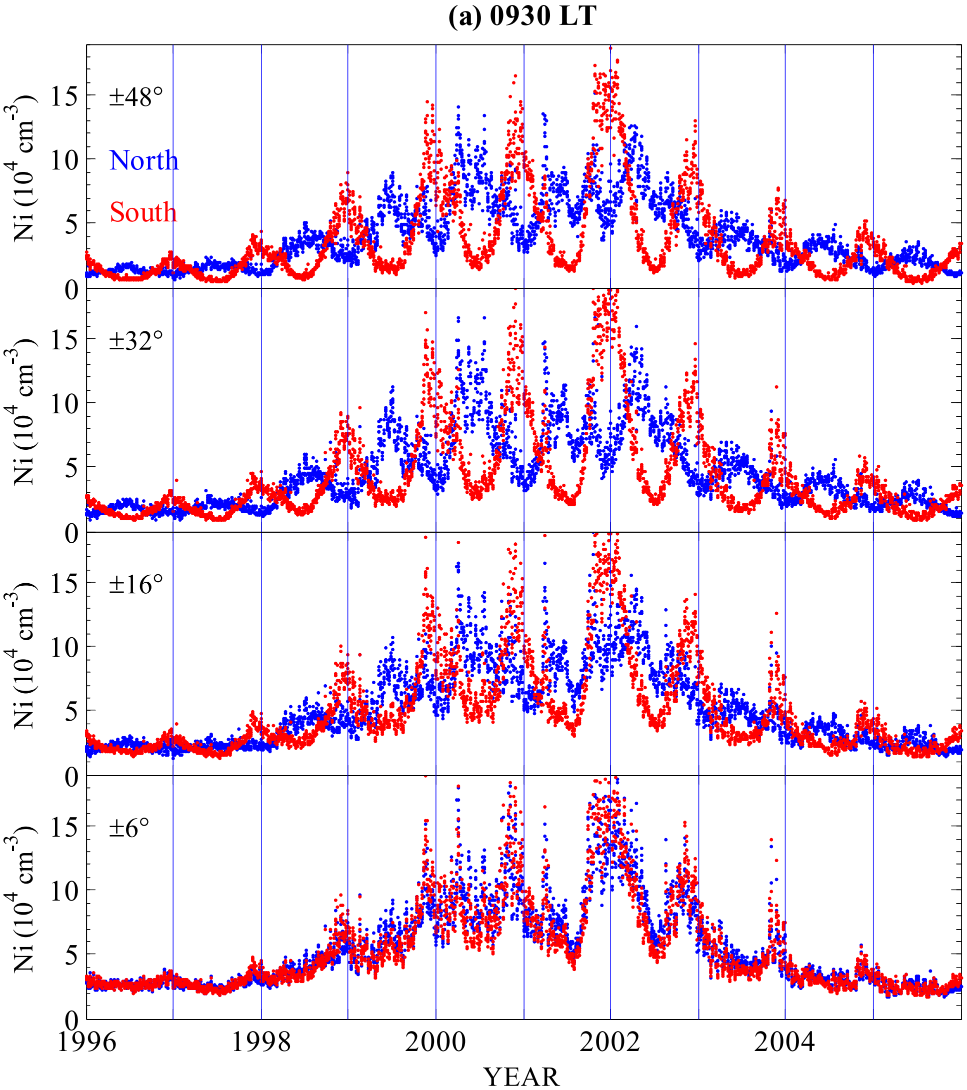

Figure 2. The longitude-averaged DMSP total ion density (N_i) during 1996–2005 at magnetic latitudes ±6°, ±16°, ±32°, and ±48° at (a) 0930 LT and (b) 2130 LT. Red dots refer to data in the Southern Hemisphere, and blue dots refer to data in the Northern Hemisphere. The vertical dashed lines show the beginnings of the years.

respectively. ε is the corresponding residual term. Because of the varying solar activity during the period under consideration and the strong solar activity effects in N_i, we further expand the above three components in equation (1) as follows:

$$\begin{aligned} A_{\mathrm{mean}} &= A_{00} + A_{01}F_{10.7}, \\ A_{\mathrm{annual}} &= (c_{10} + c_{11}F_{10.7})\cos\frac{2\pi d}{365.25} \\ &\quad + (s_{10} + s_{11}F_{10.7})\sin\frac{2\pi d}{365.25}, \\ A_{\mathrm{semiannual}} &= (c_{20} + c_{21}F_{10.7})\cos\frac{4\pi d}{365.25} \\ &\quad + (s_{20} + s_{21}F_{10.7})\sin\frac{4\pi d}{365.25}. \end{aligned} \tag{2}$$

Here $F_{10.7}$ is the solar 10.7-cm flux index, d is the day number which is counted as 1 on 1 January and 365(366) on 31 December. The amplitudes and phases of the components at any given solar activity level can be reconstructed from coefficients (c_{ij} and s_{ij}, here i = 1, 2; j = 0, 1) in equation (2) through fitting the N_i data using equation (1) with a least squares method; that is, at a given solar activity level $F_{10.7}$, the amplitude of the ith component is $\sqrt{(c_{i0} + c_{i1}F_{10.7})^2 + (s_{i0} + s_{i1}F_{10.7})^2}$ and the phase of the ith component is atan $\left(\frac{s_{i0}+s_{i1}F_{10.7}}{c_{i0}+c_{i1}F_{10.7}}\right)$. Then the phases are presented in units of day number when the maximum of N_i occurs. Figure 3 plots results normalized at two levels of solar activity corresponding to 10.7-cm flux values of $F_{10.7}$ =100 (low solar activity case) and $F_{10.7}$ = 180 (high solar activity case). The vertical axis of Figure 3 shows the magnetic latitude and the horizontal axis denotes the values of the phases (top panels) or the amplitudes (bottom panels) of the components.

[13] As shown in Figure 3, the latitudinal structure of the yearly average of N_i presents a dome-like distribution with a

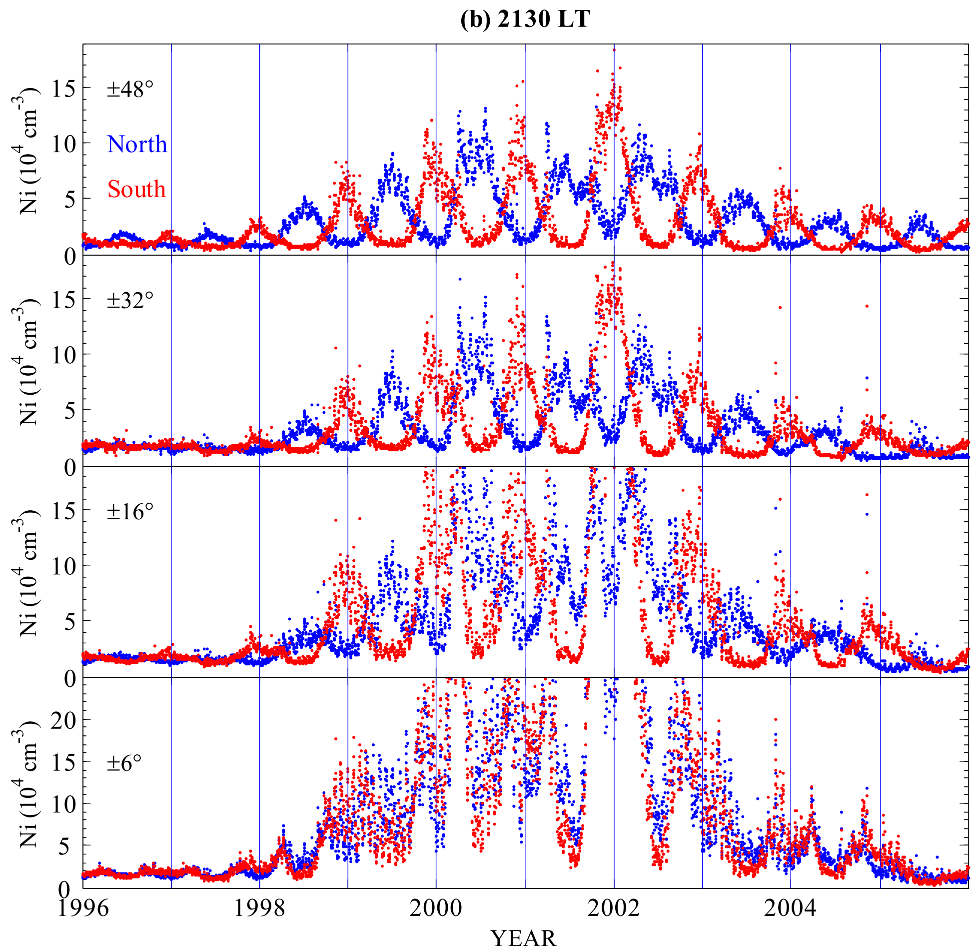

Figure 2. (continued)

maximum near the magnetic equator, which is similar to the mean term of N_i in the empirical orthogonal analysis made by *Zhao et al.* [2005]. This configuration is mainly affected by geomagnetic and solar control. At equatorial and low latitudes, the yearly averages of N_i at 2130 LT are much higher than those at higher latitudes and in the morning sector. This feature is suggested to be due to the effect of the prereversal enhancement of upward drift as discussed by *Zhao et al.* [2005].

[14] At most latitudes, the annual component dominates with amplitude stronger than that of the semiannual component. Exception occurs in a narrow latitudinal range in the northern equatorial zone (see the bottom panels in Figure 3) at which the amplitude of the semiannual component is higher than that of the annual component at the higher level of solar activity ($F_{10.7}$ = 180) at 0930 LT and for all solar activity levels at 2130 LT. The amplitudes of the annual component at both 0930 and 2130 LT increase gradually with increasing solar activity. The annual amplitudes peak near the magnetic equator in the evening sector at two levels of solar activity. In the morning sector, there are two crests at 30°S and 30°N and a trough around 10°N for $F_{10.7}$ = 180 and only a minimum around 10°N for $F_{10.7}$ = 100. Poleward of 30°S, the annual component has a much weak latitudinal variation. It is obvious that the annual component maximizes near the December solstice in the Southern Hemisphere and near the June solstice at northern middle latitudes. The phase of the annual variations varies little with latitude in the Southern Hemisphere and middle latitude in the Northern Hemisphere except that the phase shift in the annual component occurs at latitude from near the magnetic equator to low latitude in the Northern Hemisphere. An interesting feature is that, at the higher solar activity level ($F_{10.7}$ = 180), the annual phase in the Northern Hemisphere shifts from the June solstice toward May in the morning sector (see the top-left panel of Figure 3).

3.2. N_i at Solstices

[15] A more complete picture of N_i in the June solstices (averaged ±15 days centered on 21 June in each year) and the December solstices (averaged ±15 days on 21 December in each year) over the latitude range (60°N–60°S) under consideration is illustrated in Figure 4. The solid curves in Figure 4 refer to the June solstice results, while the dashed ones give the December solstice results. The plasma densities at 840 km have their highest values over a narrow latitude range around the magnetic equator. At higher latitudes, plasma densities are found to decrease with increasing latitude in both hemispheres and N_i is higher in the summer hemisphere. The maximum of N_i in the Southern Hemisphere during the December solstice is larger

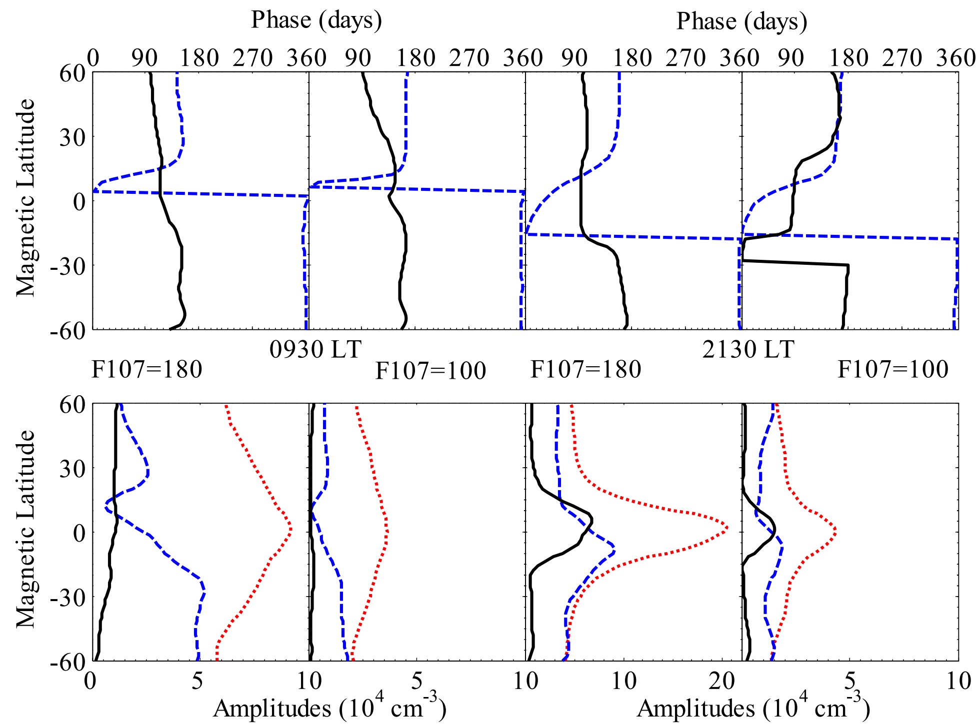

Figure 3. The amplitudes and phases of DMSP total ion density (N_i) as a function of magnetic latitude at 0930 and 2130 LT under two levels of solar activity ($F_{10.7}$ = 100 and 180). Note that the horizontal scale for the amplitudes at 2130 LT under $F_{10.7}$ = 180 is different from the other three cases. The red dotted curves denote the annual mean component, the blue dashed curves for the annual component, and the black for the semiannual component.

than that in the Northern Hemisphere during the June solstice. For each year, except a narrow latitude zone equatorial from the magnetic equator to the northern side, the month-averaged N_i is seen to be greater in local summer (June solstice for the Northern Hemisphere and December solstice for the Southern Hemisphere) than in local winter. This feature is contrary to the behavior of N_mF_2 in the F region [*Torr and Torr*, 1973]. Furthermore, at most latitudes, the latitudinal variations in any given season become particularly enhanced with increasing solar activity.

[16] The dash-dot curves in Figure 4 show the absolute differences of N_i at both the December and June solstices. The differences of N_i at the two solstices are small under low solar activity while they become much marked during the years at high levels of solar activity and reach their maximum in the years of 2000 and 2001 at most latitudes. An interesting feature is that the differences in N_i at the two solstices depend on latitude, are not symmetrical about the magnetic equator, and are generally stronger in the Southern Hemisphere than in the Northern Hemisphere. This feature is similar to that in N_e at 600-km altitude [*Bailey et al.*, 2000; *Su et al.*, 1998] and also contrary to that in N_mF_2. For example, *Torr and Torr* [1973] found that differences in N_mF_2 at the two solstices are stronger in the Northern Hemisphere than in the Southern Hemisphere.

[17] In the morning sector (0930 LT), N_i averaged at both hemispheres are substantially greater at the December solstices than at the June solstices. The differences are small in low solar activity years (1996, 2004, and 2005) while they become much greater and have a stronger latitude variation in high solar activity years (2000 and 2001). In the evening sector (2130 LT), the behavior also depends on the solar activity level. N_i is seen to be greater in the December solstices than in the June solstices at all latitudes in years from 1997 to 2002; while in 1996, 2003, 2004, and 2005, N_i at the two solstices are comparable to each other.

3.3. Annual Asymmetry Index

[18] To give a quantitative description of the annual asymmetry, we introduce the annual asymmetry index (AI) of *Mendillo et al.* [2005] at any given magnetic latitude q as given by

$$\mathrm{AI} = \frac{(N_i^N + N_i^S)_{\mathrm{December}} - (N_i^N + N_i^S)_{\mathrm{June}}}{(N_i^N + N_i^S)_{\mathrm{December}} + (N_i^N + N_i^S)_{\mathrm{June}}} \quad (3)$$

where superscripts N and S denote N_i at north and south magnetic latitudes q.

[19] To faithfully represent the annual asymmetry, we also choose the year of 2002 as done in the work of *Mendillo et al.* [2005]. The 31-day mean of $F_{10.7}$ is 153.4 for the June solstice and 152.3 for the December solstice. Figure 5 shows the latitudinal variations of AI for the longitude-averaged N_i in the year 2002. Apart from the latitudinal variation, the first feature to note is that AI illustrates a globally mean positive annual asymmetry

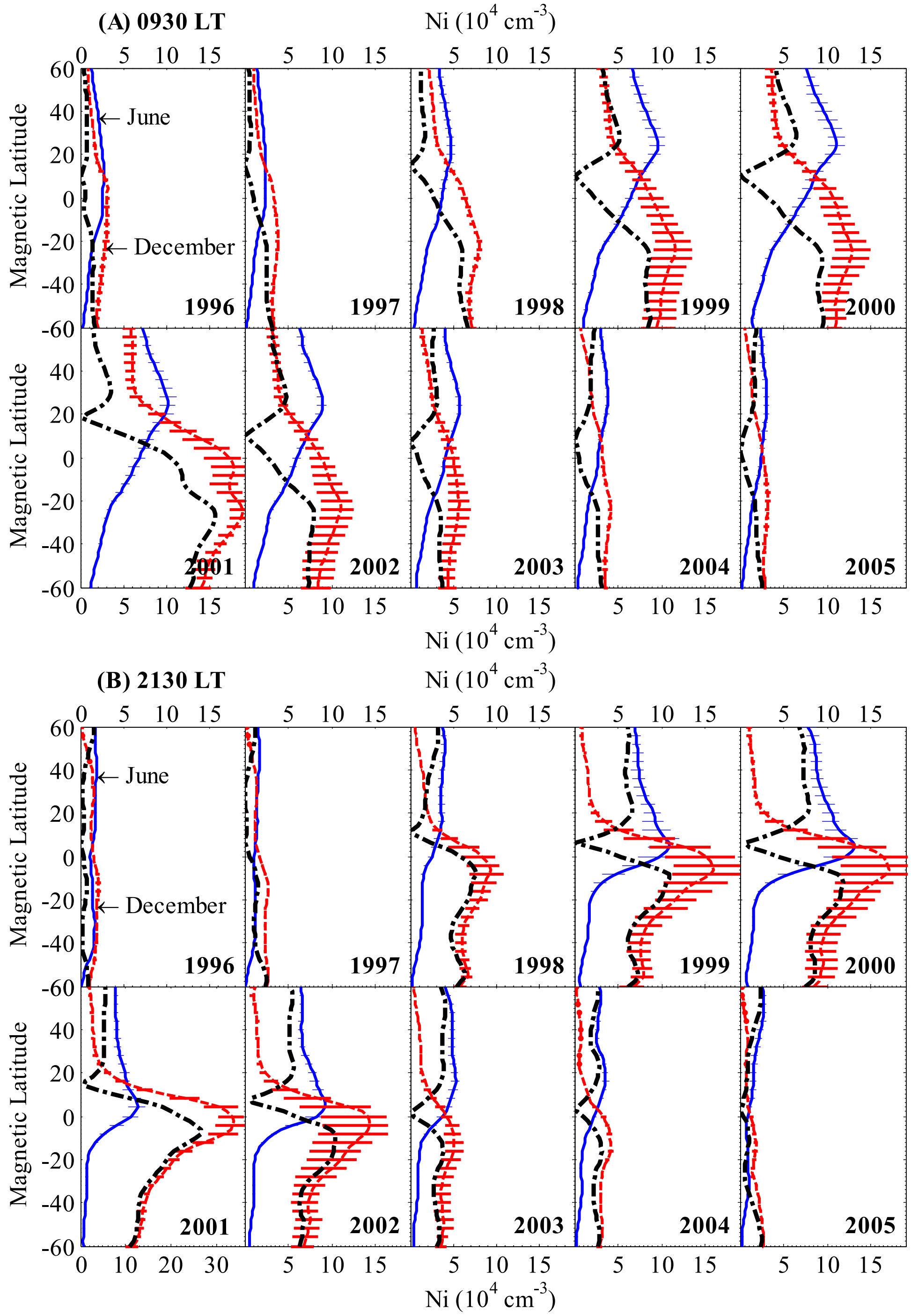

Figure 4. Longitude-averaged DMSP total ion density (N_i) as a function of magnetic latitudes at (a) 0930 LT and (b) 2130 LT at December (red dash curves) and June (blue solid curves) solstices from 1996 to 2005. The dash-dot curves correspond to the absolute differences of N_i between the two solstices. Note that the horizontal scale at 2130 LT 2001 is different from the others. The horizontal bars cover lower quartile through median values to upper quartile.

pattern. Second, AI has local time and latitude variations. The values of AI range from 0.12 to 0.22 at 0930 LT and from 0.007 to 0.285 at 2130 LT. The longitude-averaged AI in the morning sector has a minimum at low latitude (26°) and becomes larger at lower and higher latitudes while, in the evening sector, it has a peak at latitude 6° and decreases with increasing latitude up to 40°. At higher latitudes, the values of AI have an insignificant latitude variation.

3.4. Longitudinal Effect of the Annual Asymmetry of N_i

[20] The topside ionosphere shows a strong longitude effect [e.g., *Su et al.*, 1996; *Sultan and Rich*, 2001;

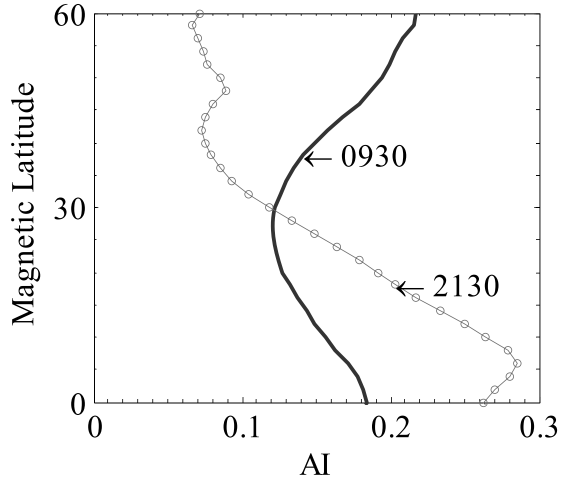

Figure 5. The annual asymmetry index AI (see text) of longitude-averaged N_i as a function of magnetic latitude at 0930 and 2130 LT in 2002.

Venkatraman and Heelis, 2000]. To investigate the longitudinal effects of the annual variations, we separately average the data over four longitude sectors at (1) 30°E, (2) 120°E, (3) 210°E, and (4) 285°E with a bandwidth ±27° and calculate the corresponding AI. The choice of longitudes for each longitude sector is based on the configuration of the geomagnetic field [see *Su et al.*, 1996]: At longitudes 30° and 120°E, the magnetic equator shifts to 10° north from the geographic equator and the magnetic declination is westward at 30°E and is small at 120°E. In contrast, the magnetic equator coincides with the geographic equator at 210°E while the former shifts to higher than 10°S geographic at 285°E.

[21] Figure 6 shows the latitudinal variations of AI in these four longitude sectors at 0930 and 2130 LT. A notable feature seen in Figure 6 is the existence of the longitude effects of the annual asymmetry which depends on local time. The longitude effects of AI are much stronger in the evening sector than in the morning sector. In the morning sector, AI keeps positive in all longitude sectors but has slightly different latitude structures in these longitude sectors. On the other hand, at 2130 LT, AI at middle latitudes becomes negative in the 30° and 120° longitude sectors, which is quite deviated from the global averaged case (Figure 5).

4. Discussion

[22] The preceding analysis reveals valuable climatological features of the topside total ion density at 840-km altitude. Among these features, the yearly variations show significant annual variations and annual asymmetry, which has strong solar activity modulations and latitudinal dependence. Obviously, the annual asymmetry exists not only in the rising phase of the solar cycle but also in the declining phase. Thus the differences in solar conditions in the two

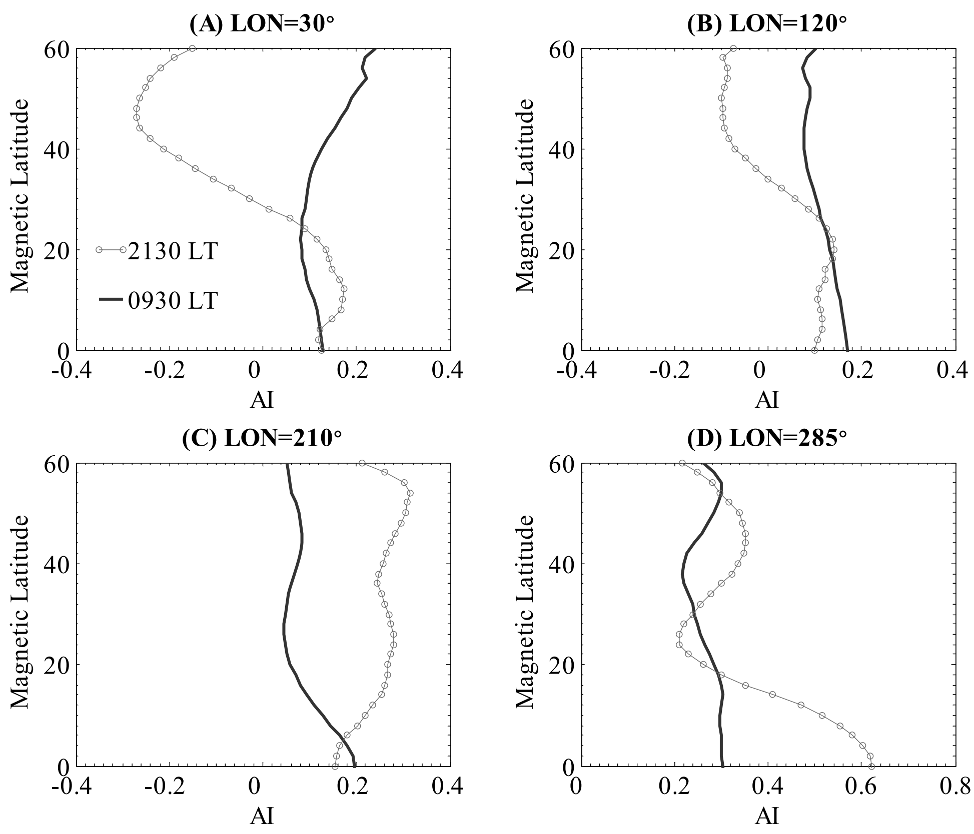

Figure 6. The annual asymmetry index AI (see text) of N_i in the four longitude zones of (a) 30° ± 27°, (b) 120° ± 27°, (c) 210° ± 27°, and (d) 285° ± 27° as a function of magnetic latitude at 0930 and 2130 LT in 2002.

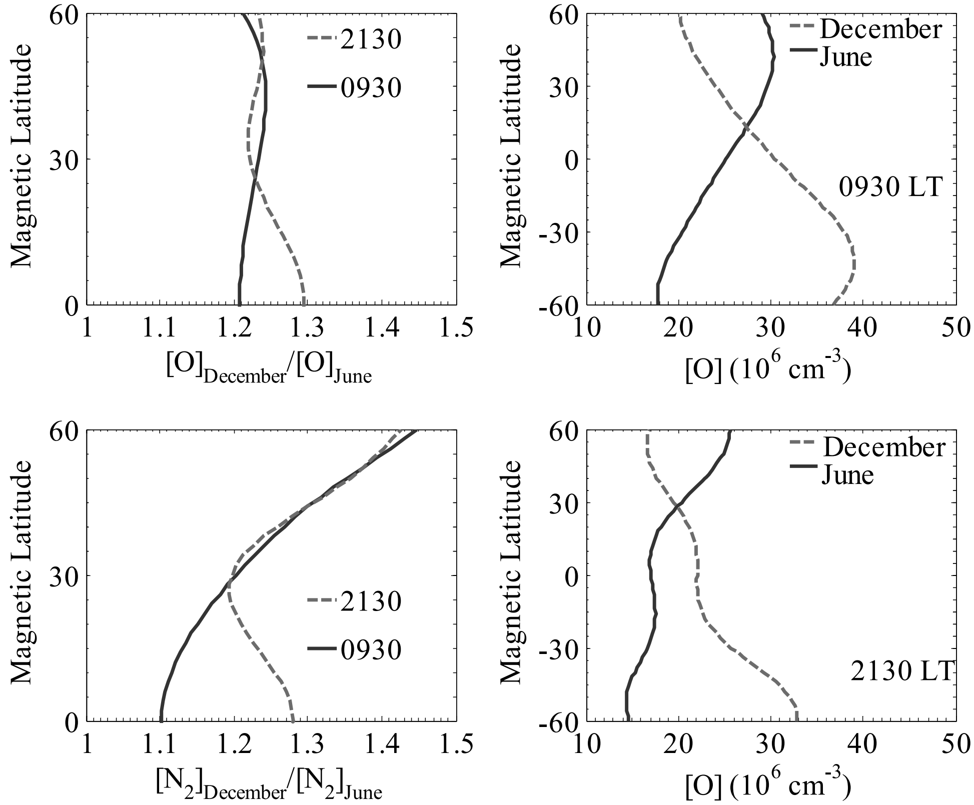

Figure 7. Right panels illustrate the concentrations of globally averaged neutral oxygen [O] in the December and June solstice at 0930 and 2130 LT in 2002. Left panels plot the ratio of conjugate averaged [O] (top) and molecular nitrogen [N_2] (bottom) in the December solstice to those in the June solstice in 2002. The input altitude used for the NRLMSISE-00 model was 500 km.

solstices do not account for the observed differences in annual asymmetry in conjugate-averaged N_i. Moreover, as mentioned by *Rishbeth and Müller-Wodarg* [2006], the possible cause of the annual asymmetry in the solstice variation in Sun-Earth distance and the consequent 7% variation in the flux of ionizing radiation cannot account for the observed solstice difference in global N_mF_2. It is also true for DMSP N_i.

4.1. Neutral Compositions

[23] There are complicated couplings between the plasma in the topside ionosphere and that at underlying altitudes and also with the neutral compositions. We find the annual asymmetry in the neutral compositions. First, we examine neutral compositions which output from the NRLMSISE-00 model [*Picone et al.*, 2002]. The right panels of Figure 7 illustrate the globally averaged concentrations of atomic oxygen [O] at 500 km in the December and June solstices at 0930 and 2130 LT in 2002, while the left panels of Figure 7 show the ratio of conjugate-averaged [O] and [N_2] in the December solstice to those in the June solstice. It is seen in Figure 7 that, according to the NRLMSISE-00 model, the conjugate-averaged values of [O] at 0930 and 2130 LT are substantially higher at the December solstices than at the June solstice and the December/June concentration ratio is 1.2–1.3. This is consistent with the satellite orbit analysis at an altitude of 470 km by *King-Hele and Walker* [1969]. A similar feature was also reported in the work of *Mendillo et al.* [2005] and in monograph [e.g., *Ivanov-Kholodny and Mikhailov*, 1986]. Moreover, the differences in [O] at the two solstices have little altitude variation at altitudes from 500 to 840 km. Thus we only show results at 500 km for typical example. Another feature that can be seen in Figure 7 is that the differences in [O] at the two solstices are larger in the Southern Hemisphere than in the Northern Hemisphere. This pattern is also consistent with that of N_i (Figure 4). On the other hand, conjugate-averaged [N_2] and [O_2] also increase higher at the December solstice, compared to the June solstices. However, the amount of atomic oxygen exceeds that of N_2 and O_2 by more than 2 orders of magnitude, thus the topside ionosphere is no longer in chemical equilibrium. Although the [O]/[N_2] ratio is always used as an indicator in discussing the *F*-layer problems, [N_2] and [O_2] falloff more rapidly with height than does [O]. This fact implies that the recombination processes related with N_2 and O_2 should be of minor importance with increasing altitude. As a result, what is important and suitable for understanding the topside annual asymmetry is the seasonal effects in [O], not the [O]/[N_2] ratio. Thus, if there is any counterpart in the neutral compositions of the atmosphere, the topside annual asymmetry should come from the annual variation of [O] rather than from that of [O_2] and [N_2]. Although there is a difference in their latitudinal patterns, the neutral composition counterpart in [O] is

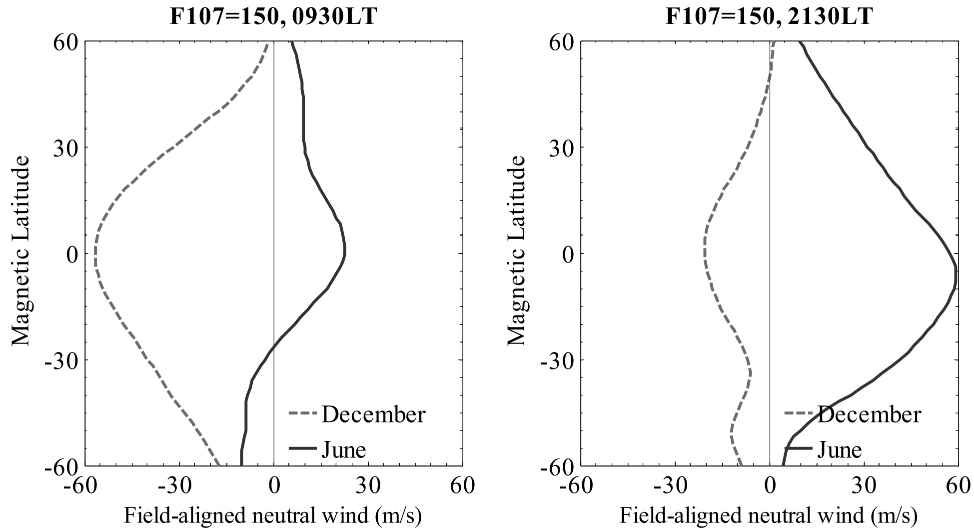

Figure 8. The field-aligned component of neutral winds from HWM-93 model in the December and June solstices in 2002. Positive values for field-aligned component of winds in the southward direction. The model winds have been averaged in longitude, and the input altitude used for the wind model was 500 km.

consistent with that in the topside plasma density. However, it should be noted that the NRLMSIS model may fail to precisely reproduce the actual latitude pattern [*Liu et al.*, 2005, 2007a].

[24] Previous modeling studies have shown that the above increase in [O] will increase the production rate of ions, which in turn increase the ion and electron densities. For instance, *Su et al.* [1998] reported their model simulation results for the 600-km ionosphere, which confirms the importance of the annual asymmetry of [O] in that of plasma densities at 600 km. Their results can also be applied to the case at 840 km if we assume topside plasma under diffusive equilibrium [*Rishbeth and Garriott*, 1969]. Thus the annual asymmetry at 840 km is at least partially explained by changes in [O] if the winds and other dynamic processes do not significantly distort the diffusive distribution of the topside plasma.

4.2. Neutral Winds

[25] It is well known that the plasma distribution in the topside ionosphere is controlled both by dynamics and by chemistry. Actually, the topside ionosphere is not in photochemical equilibrium and transport becomes the principal process. The dynamic processes of the region involve neutral winds, $E \times B$ drifts, and diffusions. Thus, besides neutral compositions, the seasonal variations of neutral winds should play an important role in the strong annual variations of N_i. Thermospheric winds push plasma up and down geomagnetic field lines and transport plasma from one hemisphere to the other by modulating the field-aligned flows [e.g., *Heelis et al.*, 1990; *Venkatraman and Heelis*, 2000], which influences the ion density latitude structure [*Oyama and Watanabe*, 2004; *Sultan and Rich*, 2001; *Watanabe et al.*, 1995] and the observed hemispheric asymmetries [*Greenspan et al.*, 1994]. Neutral winds in the magnetic meridian include contributions from both the geographic zonal and meridional winds, which depend on the magnetic declination angle. Therefore the field-aligned flows due to neutral winds may be a primary cause of the latitudinal and longitudinal dependences and the seasonal variations of the topside plasma densities [*Su et al.*, 1998; *Venkatraman and Heelis*, 2000]. Evidences can be found in the longitudinal effects of the interhemispheric plasma flows in the topside ionosphere [e.g., *Venkatraman and Heelis*, 2000]. Furthermore, it is expected that the zonal wind has significant contributions at longitudes with a significant magnetic declination [*Liu et al.*, 2004], giving the hemispheric asymmetries a longitudinal dependence [*Heelis and Hanson*, 1980; *Su et al.*, 1996; *Venkatraman and Heelis*, 2000]. As a result, the hemispheric and annual asymmetries present longitude and latitude features if neutral winds play an important role in the topside ionosphere.

[26] Let us now examine outputs from the HWM-93 neutral wind model [*Hedin et al.*, 1996]. The input altitude used for the HWM-93 model was 500 km in considering the insignificant altitude variation due to huge viscous effects at high altitudes.

[27] Figure 8 shows the field-aligned component of neutral winds from the HWM-93 model in the two solstices (solid line for the June solstice and dashed line for the December solstice) at 0930 and 2130 LT in 2002. Values of the field-aligned component of neutral winds are longitude-averaged, which is positive for southward. The influence of season on winds is that a strong field-aligned component blows from the summer hemisphere to the winter one. Thus neutral winds lift the *F* region upwards/downward in the summer/winter hemisphere so that the electron density tends to increase/decrease in the summer/winter hemisphere [*Rishbeth*, 1998]. This change will couple to regions at higher altitudes [*Guiter et al.*, 1995]. As a result, topside N_i has a higher value in the summer hemisphere than in the winter hemisphere and is asymmetrical about the magnetic equator. This has been used to derive information of neutral winds by *Sultan and Rich* [2001].

[28] Furthermore, as shown in Figure 8, there is a pronounced difference between the December solstice and the June solstice. For example, at 0930 LT, the December solstice winds are northward for both hemispheres, and the June solstice winds are southward in the Northern Hemisphere and southern low latitude, but they turn to northward in the South Hemisphere with magnetic latitudes higher than 28°S. We know that equatorward winds tend to push plasma to higher altitude, where the loss rate is smaller. As a result, higher density will also be resulted. From the difference of winds for both solstices, the net effect of the difference in winds will cause the plasma density to be higher in the Southern Hemisphere. It is interesting that the pattern of this difference is also constituent with a larger difference of N_i during the two solstices in the Southern Hemisphere (Figure 4).

5. Summary

[29] This paper has analyzed the 10-year (1996–2005) measurements of total ion density (N_i) from the Defense Meteorological Satellite Program (DMSP) spacecraft at 0930 and 2130 LT to investigate the yearly variations of global topside plasma densities within ±60° magnetic latitude. In summary, the major findings are outlined as follows.

[30] 1. The total ion densities at 840-km altitude show strong yearly variations with local time, longitude and latitude structures, and solar activity modulation.

[31] 2. The annual components dominate in the yearly variations of longitude-averaged N_i at most latitudes with maxima around the June solstices in the Northern Hemisphere and around the December solstices in the Southern Hemisphere. Moreover, the differences in N_i at the two solstices are not symmetrical about the magnetic equator, being generally stronger in the Southern Hemisphere than in the Northern Hemisphere. Exception occurs in the northern equatorial zone, where seasonal anomaly still exists with N_i, being maxima N_i around the December solstices. In contrast, significant semiannual anomaly is seen in the plasma densities at 600 km and in the ionospheric *F* region [e.g., *Bailey et al.*, 2000; *Balan et al.*, 2000] and TEC [*W. Wan, et al.*, submitted manuscript, 2007].

[32] Conjugate-averaged N_i at both hemispheres is substantially greater at the December solstices than at the June solstices at most latitudes. The solstice differences and annual asymmetry are more distinctly manifested with increasing solar activity.

[33] The annual asymmetry has latitudinal and longitudinal structures and is modulated by solar activity effect. The values of annual asymmetry index (AI) range from 0.12 to 0.22 at 0930 LT and from 0.007 to 0.285 at 2130 LT. The longitude effects of the annual asymmetry depend on local time, being stronger in the evening sector than in the morning sector.

[34] The annual asymmetry in N_i cannot be explained by the solar condition differences between the two solstices. The changes of neutral oxygen concentration [O] from the NRLMSIS model show a similar asymmetry and the hemispheric pattern as N_i. Moreover, effects of the HWM model neutral winds are consistent with the change patterns of N_i. Thus the effect of annual anomaly may be explained in terms of the different changes of [O] and neutral winds in upper atmosphere at the December and June solstices.

[35] To understand the detailed physical processes involved, diagnostic runs with a coupled thermosphere-ionosphere modeling is highly desirable. Furthermore, this investigation supports the existence of altitude dependence of the yearly variations. To understand their features, more research should be conducted on observations from other altitudes.

[36] **Acknowledgments.** The authors thank the referees for their valuable suggestions to the paper. The DMSP data are provided by the Center for Space Sciences at University of Texas at Dallas and the US Air Force. The $F_{10.7}$ index is taken from the SPIDR Web site. This research was supported by the National Natural Science Foundation of China (40674090, 40636032), the KIP Pilot Project (kzcx3-sw-144) of Chinese Academy of Sciences, and National Important Basic Research Project (2006CB806306).

[37] Amitava Bhattacharjee thanks the reviewers for their assistance in evaluating this paper.

References

Bailey, G. J., Y. Z. Su, and K.-I. Oyama (2000), Yearly variations in the low-latitude topside ionosphere, *Ann. Geophys.*, *18*, 789–798.

Balan, N., Y. Otsuka, G. J. Bailey, and S. Fukao (1998), Equinoctial asymmetries in the ionosphere and thermosphere observed by the MU radar, *J. Geophys. Res.*, *103*(A5), 9481–9495.

Balan, N., Y. Otsuka, S. Fukao, M. A. Abdu, and G. J. Bailey (2000), Annual variations of the ionosphere: a review based on MU radar observations, *Adv. Space Res.*, *25*(1), 153–162.

Denton, M. H., G. J. Bailey, Y. Z. Su, K. I. Oyama, and T. Abe (1999), High altitude observations of electron temperature and a possible north-south asymmetry, *J. Atmos. Sol. Terr. Phys.*, *61*, 775–788.

Duncan, R. A. (1969), F-region seasonal and magnetic storm behaviour, *J. Atmos. Terr. Phys.*, *31*, 59–70.

Fatkullin, M. N. (1973), Storms and the seasonal anomaly in the topside ionosphere, *J. Atmos. Terr. Phys.*, *35*, 453–468.

Gondhalekar, P. M., and J. W. King (1973), The latitudinal variation of the electron concentration in the topside ionosphere in winter, *J. Atmos. Terr. Phys.*, *535*, 1299–1308.

Greenspan, M. E., W. J. Burke, F. J. Rich, W. J. Hughes, and R. A. Heelis (1994), DMSP F8 observations of the mid-latitude and low-latitude top ionosphere near solar minimum, *J. Geophys. Res.*, *99*, 3817–3826.

Guiter, S. M, C. E. Rasmussen, T. I. Gombosi, J. J. Sojka, and R. W. Schunk (1995), What is the source of observed annual variations in plasmaspheric density?, *J. Geophys. Res.*, *100*(A5), 8013–8020.

Gulyaeva, T. L., and K. Rawer (2003), North\south asymmetry of the equatorial anomaly: A model study, *Adv. Space Res.*, *31*(3), 549–554.

Hedin, A. E., E. L. Fleming, A. H. Manson, et al. (1996), Empirical wind model for the upper, middle and lower atmosphere, *J. Atmos. Terr. Phys.*, *58*(13), 1421–1447.

Heelis, R. A., and W. B. Hanson (1980), Interhemispheric transport induced by neutral zonal winds in the F-region, *J. Geophys. Res.*, *85*, 3045–3047.

Heelis, R. A., W. B. Hanson, and G. J. Bailey (1990), Distributions of the He+ at middle and equatorial latitudes during solar maximum, *J. Geophys. Res.*, *95*, 10,313–10,320.

Huang, C. Y., W. J. Burke, J. S. Machuzak, L. C. Gentile, and P. J. Sultan (2001), DMSP observations of equatorial plasma bubbles in the topside ionosphere near the solar maximum, *J. Geophys. Res.*, *106*(A5), 8131–8142.

Ivanov-Kholodny, G. S., and A. V. Mikhailov (1986), *The Prediction of Ionospheric Conditions*, 167 p., Springer, New York.

King-Hele, D. G., and D. M. C. Walker (1969), Air density at a height of 470 km between January 1967 and May 1968, from the orbit of the satellite 1966-118A, *Planet. Space Sci.*, *17*, 197–215.

Liu, L., X. Luan, W. Wan, J. Lei, and B. Ning (2004), Solar activity variations of equivalent winds derived from global ionosonde data, *J. Geophys. Res.*, *109*, A12305, doi:10.1029/2004JA010574.

Liu, H., H. Lühr, V. Henize, and W. Köhler (2005), Global distribution of the thermospheric total mass density derived from CHAMP, *J. Geophys. Res.*, *110*, A04301, doi:10.1029/2004JA010741.

Liu, H., C. Stolle, S. Watanabe, T. Abe, M. Rother, and D. L. Cooke (2006a), Evaluation of the IRI model using CHAMP observations in polar and equatorial regions, *Adv. Space Res.*, doi:10.1016/j.asr.2006.08.006.

Liu, L., W. Wan, B. Ning, O. M. Pirog, and V. I. Kurkin (2006b), Solar activity variations of the ionospheric peak electron density, *J. Geophys. Res.*, *111*, A08304, doi:10.1029/2006JA011598.

Liu, H., H. Lühr, and S. Watanabe (2007a), Climatology of the equatorial thermospheric mass density anomaly, *J. Geophys. Res.*, *112*, A05305, doi:10.1029/2006JA012199.

Liu, L., W. Wan, X. Yue, B. Zhao, B. Ning, and M.-L. Zhang (2007b), The dependence of plasma density in the topside ionosphere on solar activity level, *Ann. Geophys.*, *25*(6), 1337–1343.

Mendillo, M., C. Huang, X. Pi, H. Rishbeth, and R. Meier (2005), The global ionospheric asymmetry in total electron content, *J. Atmos. Sol. Terr. Phys.*, *67*, 1377–1387.

Millward, G. H., R. J. Moffett, S. Quegan, and T. J. Fuller-Rowell (1996), Ionospheric F2 layer seasonal and semiannual variations, *J. Geophy. Res.*, *101*, 5149–5156.

Moffett, R. J. (1979), The equatorial anomaly in the electron distribution of the terrestrial F-region, *Fund. Cosmic Phys.*, *4*, 313–391.

Oyama, K., and S. Watanabe (2004), Effects of zonal and meridional neutral winds on the electron density and temperature at the height of 600 km, *JAXA Research and Development Report*, 12 p., Japan Aerospace Exploration Agency.

Picone, J. M., A. E. Hedin, D. P. Drob, and A. C. Aikin (2002), NRLMSISE-00 empirical model of the atmosphere: Statistical comparisons and scientific issues, *J. Geophys. Res.*, *107*(A12), 1468, doi:10.1029/2002JA009430.

Rich, F. J., P. J. Sultan, and W. J. Burke (2003), The 27-day variations of the plasma densities and temperatures in the topside ionosphere, *J. Geophys. Res.*, *108*(A7), 1297, doi:10.1029/2002JA009731.

Richards, P. G. (2001), Seasonal and solar cycle variations of the ionospheric peak electron density: comparison of measurement and models, *J. Geophys. Res.*, *106*(A12), 12,803–12,819.

Rishbeth, H. (1998), How the thermospheric circulation affects the ionosphere, *J. Atmos. Sol. Terr. Phys.*, *60*, 1385–1402.

Rishbeth, H., and O. K. Garriott (1969), *Introduction to Ionospheric Physics*, 331 p., Elsevier, New York.

Rishbeth, H., and I. C. F. Müller-Wodarg (2006), Why is there more ionosphere in January than in July? The annual asymmetry in the F2-layer, *Ann. Geophys.*, *24*, 3293–3311.

Rishbeth, H., and C. S. G. K. Setty (1961), The F-layer at sunrise, *J. Atmos. Terr. Phys.*, *21*, 263–276.

Rishbeth, H., I. C. F. Müller-Wodarg, L. Zou, T. J. Fuller-Rowell, G. H. Millward, R. J. Moffett, D. W. Idenden, and A. D. Aylward (2000), Annual and semiannual variations in the ionospheric F2-layer: II. Physical discussion, *Ann. Geophys.*, *18*, 945–956.

Rüster, R., and J. W. King (1973), Atmospheric composition changes and the F2-layer seasonal anomaly, *J. Atmos. Terr. Phys.*, *35*, 1317–1322.

Su, Y. Z., K. I. Oyama, G. J. Bailey, S. Fukao, T. Takahashi, and H. Oya (1996), Longitudinal variations of the topside ionosphere at low latitudes: Satellite measurements and mathematical modelings, *J. Geophys. Res.*, *101*(A8), 17,191–17,205.

Su, Y. Z., G. J. Bailey, and K.-I. Oyama (1998), Annual and seasonal variations in the low-latitude topside ionosphere, *Ann. Geophys.*, *16*, 974–985.

Su, Y. Z., G. J. Bailey, and S. Fukao (1999), Altitude dependencies in the solar activity variations of the ionospheric electron density, *J. Geophys. Res.*, *104*(A7), 14,879–14,891.

Su, S.-Y., C. K. Chao, H. C. Yeh, and R. A. Heelis (2005), Seasonal and latitudinal distributions of the dominant light ions at 600 km topside ionosphere from 1999 to 2002, *J. Geophys. Res.*, *110*, A01302, doi:10.1029/2004JA010564.

Su, S.-Y., C. H. Liu, H. H. Ho, and C. K. Chao (2006), Distribution characteristics of topside ionospheric density irregularities: Equatorial versus midlatitude regions, *J. Geophys. Res.*, *111*, A06305, doi:10.1029/2005JA011330.

Sultan, P. J., and F. J. Rich (2001), Determination of a proxy for F region meridional neutral winds using in situ satellite ion density measurements, *J. Geophys. Res.*, *106*(A10), 21,033–21,038.

Titheridge, J. E., and M. J. Buonsanto (1983), Annual variations in the electron content and height of the F layer in the Northern and Southern Hemispheres, related to neutral compositions, *J. Atmos. Terr. Phys.*, *45*, 683–696.

Torr, D. G., M. R. Torr, and P. G. Richards (1980), Causes of the F region winter anomaly, *Geophys. Res. Lett.*, *7*, 301–304.

Torr, M. R., and D. G. Torr (1973), The seasonal behaviour of the F2-layer of the ionosphere, *J. Atmos. Terr. Phys.*, *35*, 2237–2251.

Venkatraman, S., and R. Heelis (2000), Interhemispheric plasma flows in the equatorial topside ionosphere, *J. Geophys. Res.*, *105*(A8), 18,457–18,464.

Watanabe, S., K.-I. Oyama, and M. A. Abdu (1995), Computer simulation of electron and ion densities and temperatures in the equatorial F region and comparison with Hinotori results, *J. Geophys. Res.*, *100*(A8), 14,581–14,590.

West, K. H., R. A. Heelis, and F. J. Rich (1997), Solar activity variations in the composition of the low-latitude topside ionosphere, *J. Geophys. Res.*, *102*(A1), 295–305.

Whalen, J. A. (2003), Dependence of the equatorial anomaly and of equatorial spread F on the maximum prereversal E $\times$ B drift velocity measured at solar maximum, *J. Geophys. Res.*, *108*(A5), 1193, doi:10.1029/2002JA009755.

Wright, J. W. (1963), The F-region seasonal anomaly, *J. Geophys. Res.*, *68*, 4379–4381.

Yonezawa, T. (1971), The solar-activity and latitudinal characteristics of the seasonal, non-seasonal and semi-annual variations in the peak electron densities of the F2-layer at noon and midnight in middle and low latitudes, *J. Atmos. Terr. Phys.*, *33*, 889–907.

Zhang, S.-R., J. M. Holt, A. P. van Eyken, M. McCready, C. Amory-Mazaudier, S. Fukao, and M. Sulzer (2005), Ionospheric local model and climatology from long-term databases of multiple incoherent scatter radars, *Geophys. Res. Lett.*, *32*, L20102, doi:10.1029/2005GL023603.

Zhao, B., W. Wan, L. Liu, X. Yue, and S. Venkatramn (2005), Statistical characteristics of the total ion density in the topside ionosphere during the period 1996–2004 using empirical orthogonal function (EOF) analysis, *Ann. Geophys.*, *23*, 3615–3631.

Zou, L., H. Rishbeth, I. C. F. Muller-Wodarg, A. D. Aylward, G. H. Millward, T. J. Fuller-Rowell, D. W. Idenden, and R. J. Moffett (2000), Annual and semiannual variations in the ionospheric F2-layer: I. Modelling, *Ann. Geophys.*, *18*, 927–944.

L. Liu, W. Wan, X. Yue, M.-L. Zhang, and B. Zhao, Institute of Geology and Geophysics, Chinese Academy of Sciences, Beijing 100029, China. (liul@mail.iggcas.ac.cn)

S. Venkartraman, William B. Hanson Center for Space Sciences, University of Texas at Dallas, Richardson, TX, USA.